SIAM J. APPL. MATH.
Vol. 85, No. 5, pp. 2190–2214

BEHAVIORAL PLASTICITY IN CONSUMER-RESOURCE DYNAMICS*

SHOHEL AHMED†, XIAO HAN‡, AND HAO WANG§

Abstract. Understanding the mechanisms that drive biodiversity and ecosystem resilience in a rapidly changing world requires a deeper investigation into behavioral diversity among individuals. Consistent individual differences in behavior, often referred to as animal personality, play a crucial role in shaping ecological and evolutionary dynamics, particularly in foraging behavior. Traditional approaches in behavioral and evolutionary ecology typically focus on average behavior, neglecting the significance of individual variability. This study explores the influence of consumer personality on ecological dynamics, specifically examining how variations in food availability affect behavioral strategies and ecosystem functioning. We develop a consumer-resource model that incorporates personality-dependent saturating attack rates based on the mean-field ratio of resources to consumers. The well-posedness of the model is established, and we analyze the existence and stability of all steady-state solutions. Through bifurcation analysis, we identify critical transition parameters and describe the nonlinear phenomena induced by personality-dependent attack rates. Our findings demonstrate that boldness in consumers enhances their persistence, particularly under low levels of boldness, where populations can survive even with moderate or high food supply, which was not captured in classical frameworks.

Key words. consumer-resource, behavioral plasticity, bold-shy, existence, stability analysis, bifurcation analysis

MSC codes. 34C23, 34C60, 34D05, 34D20, 37G15, 92B05, 92D25

DOI. 10.1137/24M1719037

1. Introduction.

Consistent individual differences in behavior, often described as animal personality variation, play a pivotal role in the shaping of ecological and evolutionary dynamics, particularly in the context of foraging [36, 48]. Bold individuals often engage in high-risk, high-reward scenarios, maximizing resource acquisition but increasing predation exposure. In contrast, shy individuals exhibit risk-averse strategies, prioritizing survival over immediate gain [47, 15, 34]. These behavioral tendencies are not merely individual traits but have cascading effects on population dynamics and evolutionary trajectories, influencing survival rates, reproduction, and fitness on multiple scales [31, 13]. Temporal fluctuations in food availability and predation risk further drive these behavioral responses, acting as key ecological pressures shaping population-level outcomes [24, 33]. Although temporal fluctuations of food availability are key drivers of behavioral responses, their effects in the context

*Received by the editors December 18, 2024; accepted for publication (in revised form) July 23, 2025; published electronically September 24, 2025.
https://doi.org/10.1137/24M1719037
Funding: The work of the third author was partially supported by the Natural Sciences and Engineering Research Council of Canada (Individual Discovery grant RGPIN-2020-03911 and Discovery Accelerator Supplement grant RGPAS-2020-00090) and by the Canada Research Chairs Program (Tier 1 Canada Research Chair Award).
†Department of Mathematical and Statistical Sciences, University of Alberta, Edmonton, AB T6G 2G1, Canada (shohel2@ualberta.ca).
‡Department of Mathematical and Statistical Sciences, University of Alberta, Edmonton, AB T6G 2G1, Canada; School of Mathematics and Information Sciences, East China Normal University, Shanghai, 200050 China (hxxx1256ab@163.com).
§Corresponding author. Department of Mathematical and Statistical Sciences, University of Alberta, Edmonton, AB T6G 2G1, Canada (hao8@ualberta.ca).

of consumer risk-taking behavior have rarely been explored mathematically. Strong selection pressures compel consumers to adapt their behavior to resource availability, but individual consumers can exhibit consistent behavioral differences in their responses, influenced by the specific context of predation [28, 46]. Despite the critical role of these interactions, current ecological models often overlook the nuanced contributions of personality-driven behaviors. Investigating how individual traits interact with environmental heterogeneity is essential to understand the resilience of ecosystems and inform conservation of biodiversity in changing environments [41, 3]. Some empirical results suggest that behavioral types vary in a cost-benefit trade-off, with bolder individuals gaining greater access to resources at the expense of increased risk of predation [19, 35, 1]. However, explicitly linking individual behavior to predation events in natural conditions remains challenging due to the difficulty of quantifying behavior after predation, highlighting the need for theoretical studies.

Consumer-resource interactions are central to ecological modeling, providing essential insights into population dynamics, community structure, and ecosystem functioning. These interactions, encompassing consumer-resource, herbivore-plant, and host-parasite relationships, form the foundation for understanding energy transfer and nutrient cycling within ecosystems [42, 7]. The study of consumer-resource dynamics has significantly advanced theoretical ecology by offering predictive frameworks for population responses to resource availability, environmental variability, and interspecific interactions [27, 23]. Mathematical models have played a critical role in quantifying these processes, with practical applications in conservation biology, resource management, and climate impact assessments [18, 32].

Individual variation in animal behavior, such as boldness (propensity to take risks), is widespread across taxa and significantly influences species distributions, population dynamics, species interactions, and ecological invasion potential [31, 17, 4, 37]. Despite this, empirical studies on the ecological forces maintaining such variation remain limited [2, 26]. Predation risk has emerged as a key selection pressure balancing the trade-offs of risk-taking behaviors in natural environments [20, 39]. However, quantifying predation events involving individuals with known behavioral phenotypes remains methodologically challenging [10, 26]. Theoretical and empirical models incorporating personality traits have explored their effects on consumer-resource dynamics, resource partitioning, and habitat selection [30, 44]. These models offer valuable insights but often overlook feedback mechanisms between individual behaviors and environmental variability, such as resource abundance or predation risk [33]. Traditional approaches in behavioral and evolutionary ecology tend to focus on average behaviors, neglecting the functional significance of individual differences [22, 43]. This work aims to develop an ecological model integrating consumer behavioral responses under varying food availability. The model will be empirically validated and calibrated using field data to better understand how individual variation influences consumer-resource dynamics and ecological stability.

This research employs an integrated approach combining theoretical, computational, and empirical methods. First, differential equation-based models will be developed to describe the interactions between food availability and animal behavior, as outlined in section 2. Empirical data from experimental studies will be used to parameterize and validate these models, ensuring their accuracy and relevance. In section 3, we derive conditions for the existence of specified nonlinear phenomena and analyze their implications for the dynamics of the model by studying equilibria. Section 4 focuses on investigating various bifurcations by identifying critical parameter values and the conditions under which these bifurcations occur. Numerical simulations will

TABLE 1
Description of variables and parameters of the model (2.3).

Parameter list			
Symbol	Description	Value	Reference
k	Resource carrying capacity (g)	1.2	[32]
r	Maximal growth rate of resource (d^{-1})	2.5	[32]
m	Consumer loss rate (d^{-1})	0.33	[32]
e_y	Consumer maximal production efficiency (no unit)	0.7(0.5-0.9)	[16]
h	Handling time (d)	0.25(0.2-1)	[6]
b_0	Minimum attack rate ($g^{-1}d^{-1}$)	0.2(0.01-1.2)	Fitted
a	Maximum increment of attack rate ($g^{-1}d^{-1}$)	1.5(0.2-3.5)	Fitted
c	Half-saturation constant (no unit)	1.2(0-2)	Fitted
β_R	Attack rate for model (2.1) ($g^{-1}d^{-1}$)	1.2	[32]

then explore the model dynamics under diverse environmental change scenarios in section 5. Finally, the study concludes with a discussion presented in section 6.

2. The model formulation. The Rosenzweig–MacArthur consumer-resource model that incorporates density-dependent growth for the resource and a saturating functional response for the consumer [32] is formulated as follows:

$$\begin{cases} \dfrac{dx}{dt} = rx\left(1-\dfrac{x}{k}\right) - \dfrac{\beta_R xy}{1+\beta_R hx}, \\ \dfrac{dy}{dt} = e_y \dfrac{\beta_R xy}{1+\beta_R hx} - my, \end{cases} \tag{2.1}$$

where x and y are resource and consumer densities, and the parameter details are provided in Table 1. The functional response term also known as feeding rate is given by

$$f_R(x) = \frac{\beta_R x}{1+\beta_R hx}. \tag{2.2}$$

This functional response $f_R(x)$ satisfies the fundamental properties of a functional response [25].

1. $f_R(0) = 0$, i.e., at zero resource population level, there will be no interaction between resource and consumer.
2. $f_R'(x) = \frac{\beta_R}{(1+\beta_R hx)^2}$, i.e., an increase in resource increases the feeding rate.
3. $\lim_{x\to\infty} f_R = \frac{1}{h}$, i.e., for a higher resource population level, f_R saturates.

In model (2.1), the consumer's foraging behavior via attack rate β_R is considered constant. While this formulation effectively captures the fundamental dynamics of consumer-resource interactions, it neglects the potential influence of behavioral plasticity. Risk-taking behaviors, for example, can significantly alter foraging strategies based on the densities of both consumers and resources. To account for consumers adopting risk-taking behaviors to maximize resource acquisition under fluctuating resource availability, the attack rate must be treated as a dynamic variable rather than a fixed parameter. With this in mind, we propose the following personality-driven consumer-resource model:

$$\begin{cases} \dfrac{dx}{dt} = rx\left(1-\dfrac{x}{k}\right) - \dfrac{\beta(x,y)xy}{1+\beta(x,y)hx}, \\ \dfrac{dy}{dt} = e_y \dfrac{\beta(x,y)xy}{1+\beta(x,y)hx} - my. \end{cases} \tag{2.3}$$

All constant parameters in the above model are positive, and their details are provided in Table 1. Traditionally, the attack rate, β, also referred to as the foraging rate, is modeled as a constant. However, to incorporate behavioral flexibility and capture consumer personality, we extend the model by assuming that β is a function of both resource and consumer densities, $\beta(x, y)$. We constructed $\beta(x, y)$ based on the mean-field ratio of resources to consumers, capturing the dynamic interplay between resource and consumer availability. This formulation reflects the adaptive nature of consumer behavior: when resources are scarce, consumers increase boldness to improve foraging success; when competition among consumers intensifies, the boldness function saturates as competitive costs outweigh foraging benefits. A plausible candidate for this dynamic attack rate is defined as

$$\beta(x,y) = b_0 + \frac{a}{c\left(\frac{x}{y}\right)+1} = b_0 + \frac{ay}{cx+y}, \tag{2.4}$$

where the following notation is used:

- $\beta(x, y)$: the attack rate, which varies based on consumer boldness;
- b_0: the minimum attack rate, representing the baseline for a consumer exhibiting extreme shyness;
- a: the maximum possible increment to the attack rate, corresponding to a consumer exhibiting extreme boldness;
- c: the half-saturation constant governing the boldness-based increment of the attack rate; a smaller c indicates a stronger influence of boldness, while a larger c reflects a weaker influence.

The functional response (feeding rate) for the model (2.3) is given by

$$f(x,y) = \frac{\beta(x,y)x}{1+\beta(x,y)hx}, \tag{2.5}$$

which also satisfies all the basic properties of functional response like model (2.1). Figure 1 shows the schematic diagram of attack rate $\beta(x, y)$ and functional response $f(x, y)$.[1]

Model outcomes are highly sensitive to parameter values, making accurate estimation crucial for reliable quantitative predictions within a finite time interval. A systematic approach is essential for estimating multiple parameters, and various techniques have been used in previous studies [38, 16, 40]. In this study, we applied the nonlinear least-squares method (NLS), as described in Appendix A, to estimate parameters. However, empirical studies that determine feeding rates by varying resource and consumer densities in the field remain limited, particularly in complex ecosystems such as coral reefs. Using field experimental data on herbivorous fishes and their algal resources from a near-pristine reef ecosystem [16], we fitted the feeding rate function (2.5). The resulting fits are shown in Figure 1(d), with the corresponding parameter estimates provided in Table 1. A detailed description of the fitting procedure is presented in Appendix A.

By combining the generic model (2.3) with the attack function (2.4), we derive the explicit form of our model as follows:

[1]The functions $\beta(x, y)$ and $f(x, y)$ are Lipschitz with respect to x and y in the open first quadrant, respectively. Hence, their definitions can be extended to the closure of that set by letting them be zero when either $x = 0$ or $y = 0$.

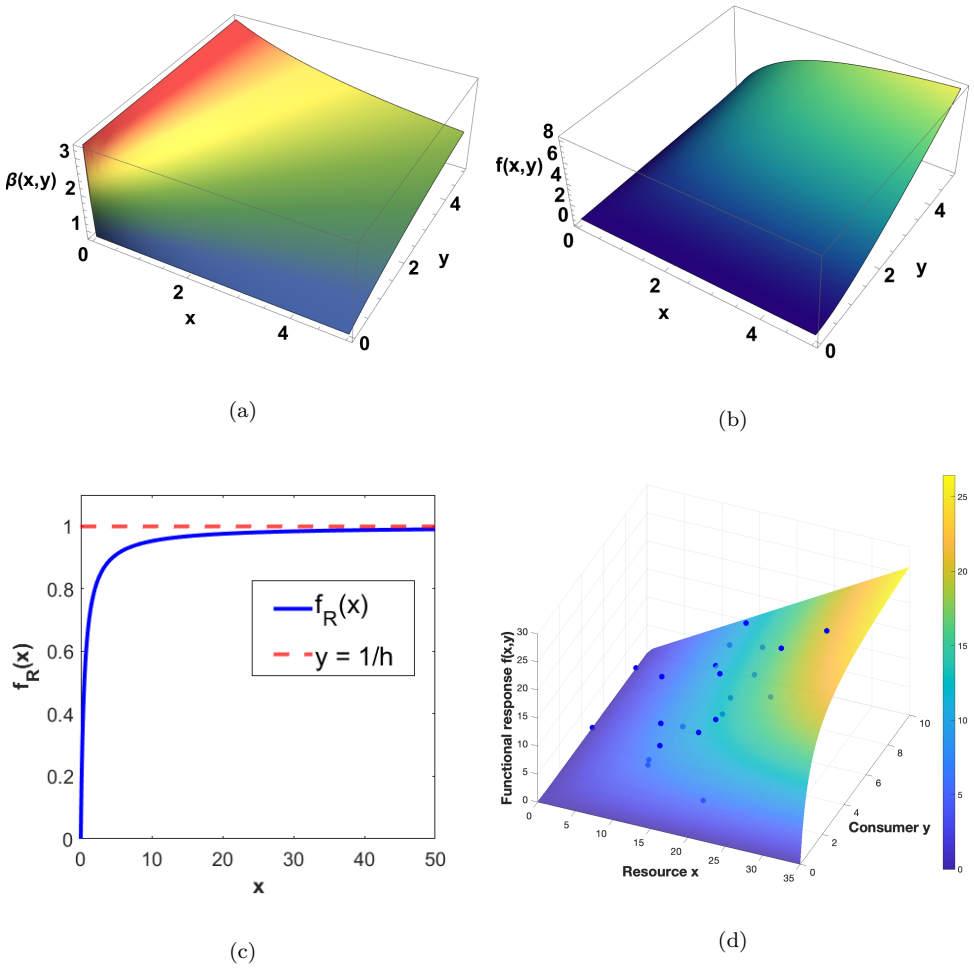

FIG. 1. *Schematic diagram for* (a) *attack rate* $\beta(x,y)$, (b) *functional response* $f(x,y)$, (c) *functional response* $f_R(x)$, *and* (d) *fitted functional response results for model* (2.3).

$$\begin{cases} \dfrac{dx}{dt} = rx\left(1-\dfrac{x}{k}\right) - \dfrac{xy\,(ay+b_0(cx+y))}{ahxy+b_0hx(cx+y)+cx+y}, \\ \dfrac{dy}{dt} = \dfrac{e_yxy\,(ay+b_0(cx+y))}{ahxy+b_0hx(cx+y)+cx+y} - m\ y. \end{cases} \tag{2.6}$$

3. Model analysis. In this section, we establish the conditions for the existence of the specified nonlinear phenomena and examine their implications for the dynamics of model (2.3).

3.1. Mathematical preliminaries. In Theorem 3.1, we demonstrate the nonnegativity and boundedness of solutions for model (2.3). The boundedness ensures the system is biologically well-behaved, preventing unbounded growth of species populations over time due to resource limitations.

THEOREM 3.1 (positivity and boundeness). *All solutions* $(x(t),y(t))$ *of the system* (2.3) *which initiate in* $\mathbb{R}^2\backslash(0,0)$ *are positive and uniformly bounded.*

Proof. The system of equations (2.3) is continuously differentiable in a neighborhood of the first quadrant $Q = \{(x, y) : x, y > 0\}$. As a result, solutions to initial value problems with nonnegative initial conditions exist and are unique. Rewrite the esystem (2.3) in the form

$$\frac{dx}{dt} = x' = x\mathcal{M}(x, y), \quad \text{and} \quad \frac{dy}{dt} = y' = y\mathcal{N}(x, y).$$

Clearly, if $(x(t), y(t))$ is a solution of the system, then $x' = xm(t)$ and $y' = yn(t)$, where $m(t) = \mathcal{M}(x(t), y(t))$ and $n(t) = \mathcal{M}(x(t), y(t))$. Hence, upon using the integration factor trick, we get $\frac{d}{dt}(e^{-\int_0^t m(s)\,ds}x(t)) = \frac{d}{dt}(e^{-\int_0^t n(s)\,ds}y(t)) = 0$, which implies

$$x(t) = e^{\int_0^t m(t)\,dt}x(0), \quad \text{and} \quad y(t) = e^{\int_0^t n(t)\,dt}y(0). \tag{3.1}$$

From (3.1), we can see that if $(x(0), y(0)) \in Q$, then $(x(t), y(t)) \in Q$, proving invariance in Q. The fundamental theorem of existence and uniqueness for differential equations guarantees that a solution curve will lie inside the first quadrant and has no intersection with the coordinate axes. Thus, the nonnegative quadrant $\mathbb{R}^2\backslash(0, 0)$ is invariant for system (2.3).

We have seen that $x(t) \geq 0$ and $y(t) \geq 0$; hence, it suffices to prove that the solutions do not cross the hypotenuse given by $x + y = \eta$. From the positivity property of our solutions, we can see that

$$x' + y' \leq rx\left(1 - \frac{x}{k}\right) - my = rx\left(1 - \frac{x}{k}\right) - m(\eta - x) = \mathcal{F}(x).$$

The maximum of the parabolic function $\mathcal{F}(x)$ on $0 \leq x$, obtained by setting its derivative to zero, is at $\bar{x} = \frac{k}{2r}(r + m)$. Hence,

$$\mathcal{F}(x) \leq \mathcal{F}(\bar{x}) = -m\eta + (m + r)\frac{k}{2r}(r + m) - \frac{r}{k}\left(\frac{k}{2r}(r + m)\right)^2 < 0$$

if η is chosen large enough. ∎

3.2. Equilibria and their stability. For an autonomous system (2.3), equilibrium points are steady state solutions. They can be determined as a solution of $\bar{F} = 0$, where $\bar{F} = [\frac{dx}{dt}, \frac{dy}{dt}]^T$. The invariant nullclines of model (2.3) represent two key scenarios: the exponential extinction of the consumer in the absence of the resource and the logistic growth of the resource in the absence of the consumer, respectively. The stability of the boundary equilibrium $E^k = (k, 0)$ is determined by the logistic dynamics of the resource when consumers are absent. The co-existing or interior equilibrium $E^* = (x^*, y^*)$ points of the system (2.3) are the points of intersection of the nullclines given by

$$\begin{cases} f_1(x, y) = r\left(1 - \dfrac{x}{k}\right) - \dfrac{\beta(x, y)y}{1 + h\beta(x, y)x} = 0, \\ f_2(x, y) = e_y\dfrac{\beta(x, y)x}{1 + h\beta(x, y)x} - m = 0. \end{cases} \tag{3.2}$$

The slope of the $f_2(x, y) = 0$ nullcline is clearly negative ($\frac{dy}{dx} < 0$), indicating that the nullcline is a decreasing function of x in the first quadrant. The nullcline $f_1(x, y) = 0$ intersects the coordinate axes at $[k, 0]$ and $[0, y_0]$, where $y_0 > 0$ is the unique solution of $y = \frac{r}{b_0 + a}$. In the first quadrant, the partial derivative

$$\frac{\partial f_1}{\partial y}(x, y) = -\frac{\beta(x, y) + hx\beta^2(x, y) + y\beta'(x, y)}{(1 + h\beta(x, y)x)^2} < 0$$

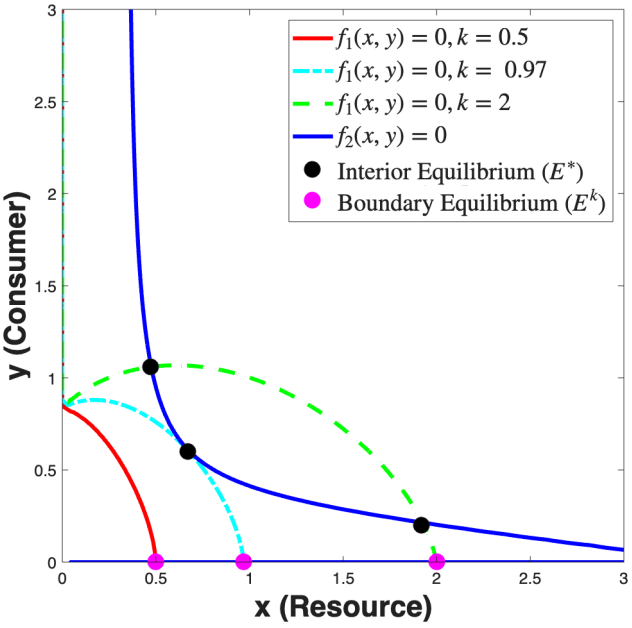

FIG. 2. *Nullclines of the system* (2.3) *for different* k *values.*

is negative, ensuring that the resource nullcline behaves as a continuous function. By the implicit function theorem, the resource nullcline remains smooth and well-defined in the first quadrant. The system (2.3) possesses an interior equilibrium point at the intersection of the nullclines within the first quadrant. From the geometric structure of the nullclines, it is evident that they either do not intersect (red curve in Figure 2) or intersect twice (green curve in Figure 2); color images are available online. Consequently, the model (2.3) either has no positive equilibrium or a pair of positive equilibria. Additionally, a transient equilibrium point of multiplicity two exists between these two system states, as illustrated by the cyan curve in Figure 2. This behavior is a general characteristic of the nullclines. Figure 2 further highlights the possible intersection patterns of the nullclines.

Letting $x^* \in (0,k)$ with $k>0$, a coexistence equilibrium E^* of system (2.3) has to satisfy

$$\begin{cases} x^* = k\dfrac{L_2}{\beta(x^*,y^*)} = k\dfrac{L_2}{\Lambda(y^*)}, \\ y^* = L_1\dfrac{\Lambda(y^*)-L_2}{\Lambda^2(y^*)}, \end{cases} \tag{3.3}$$

where $\Lambda(y^*) := \beta(x^* \in (0,k), y^*)$, $L_1 = \frac{e_y r}{e_y - hm}$, and $L_2 = \frac{m}{k(e_y - hm)}$. If $e_y - hm \le 0$, no coexistence equilibrium exists. Therefore, $e_y - hm > 0$ is a valid assumption, which also implies $L_1 > 0$ and $L_2 > 0$. That gives that the necessary condition for the existence of the positive interior equilibrium $E^* = (x^*, y^*)$ of the system (2.3) is $\Lambda(y^*) > L_2$. From the second equation of the explicit version of the model (2.6), we have

$$y = \frac{cx(m - b_0 x(e_y - hm))}{x(a+b_0)(e_y - hm) - m}.$$

That gives the same condition for the coexistence equilibrium $e_y - hm > 0$. Biologically, if the mortality rate of a consumer is less than the ratio of a conversion coefficient and handling time, then a coexistence equilibrium point becomes possible. The component x^* of the co-existing equilibrium point E^* is a root of the quadratic equation

$$a_2x^2 - a_1x + a_0 = 0. \tag{3.4}$$

Here, $a_2 = r(a+b)(e_y - hm)$, $a_1 = kr(a+b)(e_y - hm) + bkm(e_y - hm) + mr$, and $a_0 = km^2 + kmr$. Since $a_1 > 0$, the polynomial equation (3.4) can have at most two positive solutions, which correspond to the two possible co-existing equilibrium points.

THEOREM 3.2. *The consumer-only equilibrium $E^k = (k, 0)$ is locally asymptotically stable if $C_0 = \frac{e_y b_0 k}{m(1+b_0hk)} \leq 1$.*

Proof. The Jacobian matrix of the system (2.3) evaluated at $E(x, y)$ is

$$J(E) = \begin{bmatrix} a_{10} & a_{01} \\ b_{10} & b_{01} \end{bmatrix},$$

where

$$a_{10} = r - \frac{2rx}{k} - \frac{ay^3 + b_0y(cx+y)^2}{(ahxy + b_0hx(cx+y) + cx + y)^2},$$

$$a_{01} = \frac{x\left(-b_0(cx+y)\left(2ahxy + b_0hx(cx+y) + cx + y\right) - ay(ahxy + 2cx + y)\right)}{(ahxy + b_0hx(cx+y) + cx + y)^2},$$

$$b_{10} = \frac{e_y y\left(ay^2 + b_0(cx+y)^2\right)}{(ahxy + b_0hx(cx+y) + cx + y)^2},$$

$$b_{01} = \frac{e_y x\left(b_0(cx+y)\left(2ahxy + b_0hx(cx+y) + cx + y\right) + ay(ahxy + 2cx + y)\right)}{(ahxy + b_0hx(cx+y) + cx + y)^2} - m.$$

For stability, we show that all the eigenvalues of the Jacobian of the model (2.3) evaluated at the E^k have the negative real part. The Jacobian J^k evaluated at the E^k is given by

$$J^k = \begin{pmatrix} -r & -\dfrac{b_0ck^2}{b_0chk^2 + ck} \\ 0 & \dfrac{b_0e_yk}{b_0hk+1} - m \end{pmatrix}.$$

The Jacobian J^k has the following eigenvalues:

$$\lambda_1 = -r, \quad \lambda_2 = \frac{b_0e_yk}{b_0hk+1} - m.$$

Clearly, $\lambda_1 < 0$, and

$$\lambda_2 = \frac{b_0e_yk}{b_0hk+1} - m = m(C_0 - 1).$$

This implies that $\lambda_2 < 0$ if $C_0 < 1$. On the other hand, if $C_0 = 1$, $\lambda_1 = -r$ and $\lambda_2 = 0$. This also indicates that E^k is stable. The above result implies that it is possible for consumers to go extinct from the system (when $C_0 \leq 1$) if the initial size of the consumer population is in the basin of attraction of the equilibrium point E^k. ∎

Now, we show the stability of the interior equilibrium E^* of the system (2.3) in the theorem below.

THEOREM 3.3. *Consider the interior equilibrium points E_1^* and E_2^* of system (2.3). The following statements describe their local stability properties:*

1. *The interior equilibrium point E_2^*, whenever it exists, is always a saddle point.*
2. *The equilibrium E_1^* is locally asymptotically stable if the following inequality holds,*

$$\frac{ky_1^* - hmx_1^{*2}}{x_1^*} + \frac{1-(e_y - hm)x_1^*}{(\alpha y_1^* + 1)x_1^*} < 0,$$

and unstable if the expression is positive.

Proof. (1) Since we do not have the explicit expressions for the positive equilibria, we discuss their stability using the slope of nullclines at E^*. The Jacobian matrix evaluated at an interior equilibrium point $E^*(x^*, y^*)$ is given by

$$J(E^*) = \begin{bmatrix} x\dfrac{\partial f_1}{\partial x} & x\dfrac{\partial f_1}{\partial y} \\ y\dfrac{\partial f_2}{\partial x} & y\dfrac{\partial f_2}{\partial y} \end{bmatrix} = \begin{bmatrix} -x\dfrac{\partial f_1}{\partial y}\dfrac{dy^{(f_1)}}{dx} & x\dfrac{\partial f_1}{\partial y} \\ -y\dfrac{\partial f_2}{\partial y}\dfrac{dy^{(f_2)}}{dx} & y\dfrac{\partial f_2}{\partial y} \end{bmatrix}_{(x^*,y^*)}.$$

Here, $\frac{dy^{(f_i)}}{dx}$ denotes the slope of the tangent line to the curve $f_i(x,y) = 0$. Now, the determinant of the Jacobian matrix evaluated at E^* becomes

$$\mathrm{Det}(J(E^*)) = \left(xy\frac{\partial f_1}{\partial y}\frac{\partial f_2}{\partial y}\left(\frac{dy^{(f_2)}}{dx} - \frac{dy^{(f_1)}}{dx} \right) \right)_{(x^*,y^*)}. \tag{3.5}$$

Note that

$$\frac{\partial f_1(x^*,y^*)}{\partial y} = -\frac{\big(b_0(cx+y)(2ahxy+cx+y) + ay(ahxy+2cx+y) + b_0^2hx(cx+y)^2\big)}{(y(ahx+b_0hx+1)+cx(b_0hx+1))^2} < 0,$$

$$\frac{\partial f_2(x^*,y^*)}{\partial y} = \frac{e_y\big(2cxy(a+b_0)(b_0hx+1) + y^2(a+b_0)(hx(a+b_0)+1) + b_0c^2x^2(b_0hx+1)\big)}{(x(hy(a+b_0)+b_0chx+c)+y)^2} > 0.$$

Suppose that θ_1 and θ_2 are the angles of inclination of the tangents to $f_1(x,y) = 0$ and $f_2(x,y) = 0$ at E_2^*, respectively (see Figure 3). We observe that $\frac{\pi}{2} < \theta_1 < \theta_2 < \pi$ holds whenever E_2^* exists, which implies

$$\frac{dy^{(f_2)}}{dx}(x_2^*, y_2^*) > \frac{dy^{(f_1)}}{dx}(x_2^*, y_2^*).$$

Hence, we find $\mathrm{Det}(J(E_2^*)) < 0$ from (3.5) and therefore E_2^* is a saddle point.

(2) For co-existing equilibrium E_1^*, we find

$$\frac{dy^{(f_2)}}{dx}(x_1^*, y_1^*) < \frac{dy^{(f_1)}}{dx}(x_1^*, y_1^*).$$

Therefore, $\mathrm{Det}(J(E_1^*)) > 0$ and the stability of E_1^* depends on the sign of the trace of the Jacobian matrix $J(E_1^*)$:

$$\mathrm{Tr}(J(E_1^*)) = \left[x\frac{\partial f_1}{\partial x} + y\frac{\partial f_2}{\partial y} \right]_{(x_1^*,y_1^*)} = \frac{ky_1^* - hmx_1^{*2}}{x_1^*} + \frac{1-(e_y-hm)x_1^*}{(\alpha y_1^*+1)x_1^*}.$$

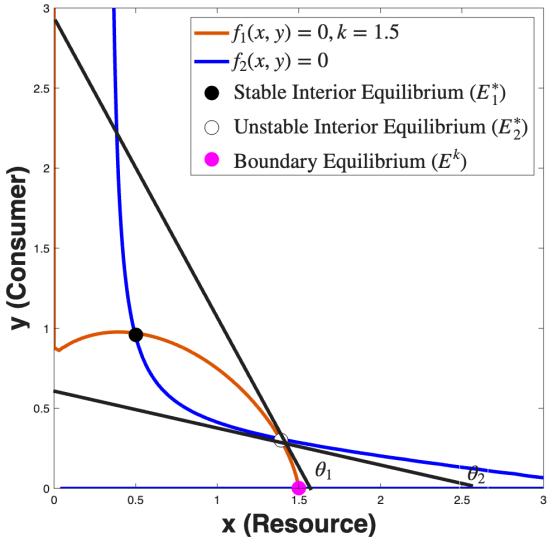

FIG. 3. *Locations of various equlibria: orange and blue color curves denote the resource and consumer nullclines, respectively.*

Therefore, E_1^* is asymptotically stable if the expression on the right-hand side is negative and unstable if it is positive. ∎

Remark 3.4. From (3.3) we get that the necessary condition for the existence of the positive interior equilibrium $E^* = (x^*, y^*)$ of the system (2.3) is $\Lambda(y^*) > L_2$, which gives $C_0 > 1$.

4. Bifurcation analysis. In this section, we examine the bifurcations of model (2.3) by identifying the critical parameter values and the conditions under which bifurcations occur. These bifurcations reveal how the system's dynamics change qualitatively in response to parameter variations, highlighting key transitions in behavior.

4.1. Fold bifurcation. From the y^* condition in (3.3), we obtain the following implicit function,

$$\mathcal{F}(y^*) := y^* \Lambda^2(y^*) - L_1(\Lambda(y^*) - L_2) = 0$$

,of the nonzero consumer equilibrium y^* (having one-to-one correspondence to the nonzero resource equilibrium x^* via (3.3)). In a limit point related to merging and disappearance of two equilibria on a fold of the equilibrium manifold, the value of y^* satisfies $\mathcal{F}'(y^*) = 0$, which can be equivalently expressed as

$$\Lambda^3(y^*) - L_1(2L_2 - \Lambda(y^*))\Lambda'(y^*) = 0. \tag{4.1}$$

Recall that $\Lambda(y)$ is smooth. In Appendix B, we show that this condition is both necessary and sufficient for vanishing of the Jacobian of the model (2.3) at a coexistence equilibrium. It is obvious that for y^* to be a limit point, it has to satisfy $\Lambda(y^*) < 2L_2$ since $\Lambda'(y^*) > 0$ and (4.1) holds. For our specific family of functional responses (2.5) we are most interested in how dynamics of the model (2.3) vary. Using the expression (2.4), the fold bifurcation manifolds can be written in polynomial form at the coexistence equilibrium $E^* = (x^*, y^*)$ $(x^* \in (0, k))$ as

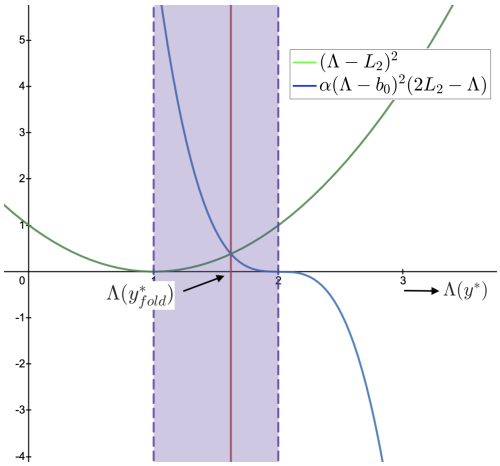

FIG. 4. *Schematic diagram for the fold bifurcation condition* (4.2).

$$(\Lambda - L_2)^2 = \alpha(\Lambda - b_0)^2(2L_2 - \Lambda), \tag{4.2}$$

where $\alpha = \frac{cm}{ae_y r}$. The fold bifurcation can be interpreted as a catastrophe when it leads to a sudden decline in the density of a threatened or exploited population, or as a benefit when it results in a sudden increase in resource density. Conversely, it can also represent a rapid population increase under certain conditions. Importantly, the shape of the fold manifold (its roots) explicitly depends on the consumer minimum attack rate (b_0), while its overall structure is influenced by other key parameters. A schematic diagram illustrating the fold bifurcation condition is provided in Figure 4.

4.2. Hopf bifurcation. The coexistence equilibrium can undergo a Hopf bifurcation, indicating a local qualitative change in the phase space. At this bifurcation point, a periodic solution either emerges from or disappears at the equilibrium as the bifurcation parameter crosses a critical value. This occurs when the real parts of both eigenvalues of the Jacobian transversally cross zero, leading to the appearance of two purely imaginary eigenvalues at the coexistence equilibrium. The necessary condition for the occurrence of a Hopf bifurcation curve at the coexistence equilibrium $E^* = (x^*, y^*)$ is

$$\Lambda' = \frac{(e_y L_2 - mh(\Lambda - L_2))\Lambda^2}{e_y m(\Lambda - L_2)}, \tag{4.3}$$

and

$$\Lambda^3 - L_1(2L_2 - \Lambda)\Lambda' > 0, \tag{4.4}$$

where $\Lambda = \Lambda(y^*)$. The condition (4.3) ensures that the trace of the Jacobian of model (2.3) vanishes at a coexistence equilibrium, and the condition (4.4) guarantees the positivity of the Jacobian at this equilibrium. In Appendix C, we prove that condition (4.3) is both necessary and sufficient for the vanishing trace of the Jacobian. Substituting Λ' from (4.3) into (4.4), the condition (4.4) can be rewritten as

$$\Lambda(\Lambda - L_2) > \eta_1(\Lambda - 2L_2)\Big(\Lambda - L_2\eta_2\Big), \tag{4.5}$$

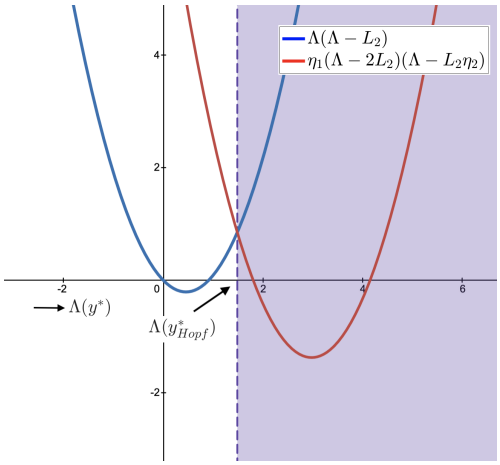

FIG. 5. *Schematic diagram for the Hopf bifurcation condition* (4.5).

where $\eta_1 = \frac{rh}{e_y - hm}$ and $\eta_2 = \frac{e_y + hm}{hm}$. A graphical representation of the inequality (4.5) is shown in Figure 5. In this figure, the convex parabolas correspond to the left-hand and right-hand sides of expression (4.5), and $\Lambda(y^*_{Hopf})$ is the unique point where they intersect. Since we are specifically considering the case of consumer-resource coexistence, where the condition $\Lambda(y^*) > L_2$ holds, it is clear that (4.5) remains valid for all $\Lambda(y^*)$ values lying between the roots of the right-hand side of expression (4.5).

We have seen that the stability of E^* depends on the sign of $\mathrm{Tr}(J(E^*))$ through condition (4.5). Here, we consider k as a bifurcation parameter. We have chosen k as the bifurcation parameter of the Hopf bifurcation but any other parameter is a valid choice. k has been chosen in order to respect traditions as the paradox of enrichment was described with respect to k [32]. Now, E^* loses its stability when the sign of $\mathrm{Tr}(J(E^*))$ changes from negative to positive due to variation of k. The co-existing equilibrium E^* of the system (2.3) undergoes a Hopf bifurcation at $k = k_{Hopf}$ if

$$\mathrm{Det}(J(E^*; k = k_{Hopf})) > 0 \quad \text{and} \quad \frac{d}{dk}\left(\mathrm{Tr}(J(E^*))\right)\Big|_{k=k_{Hopf}} \neq 0.$$

To determine the stability and direction of Hopf bifurcations near the positive equilibrium E^*, we analyze the first Lyapunov coefficient l_1 using the following theorem.

THEOREM 4.1. *Let the model* (2.3) *undergo a Hopf bifurcation at the equilibrium point* $E^*(x_1^*, y_1^*)$ *with respect to the parameter* k *at the bifurcation point* $k = k_{Hopf}$. *If the First Lyapunov coefficient* $l_1 \neq 0$, *the Hopf bifurcation is supercritical if* $l_1 < 0$, *and it is subcritical if* $l_1 > 0$, l_1 *is calculated in the proof of the theorem.*

The detailed proof of this theorem is provided in [29], and in Appendix C we give the explicit expression for l_1. Due to the lack of an explicit expression for the coexistence equilibrium E^*, determining the sign of l_1 analytically is not feasible. However, numerical analysis shows that a Hopf bifurcation occurs around $E^* = (0.32, 1.3)$ at $k_{Hopf} = 1.4$ (see Figure 8(b)). The first Lyapunov coefficient is $l_1 = -5.453 < 0$, indicating a supercritical Hopf bifurcation. In consumer-resource systems, a Hopf bifurcation signals the transition from stable coexistence to periodic oscillations, where population densities fluctuate with parameter changes. This behavior can drive populations to low levels, risking extinction. If resources vanish first, consumers collapse; if consumers vanish, resources may recover or also disappear, depending on conditions.

4.3. Transcritical bifurcation. Due to the transcritical bifurcation, a coexistence equilibrium E^* merges with the resource-only equilibrium E^K.

THEOREM 4.2 (transcritical bifurcation for E^k). *The necessary condition of transcritical bifurcation of boundary equilibrium is* E^k *is* $\beta(x^*, 0) = L_2$ *with* $x^* \in (0, k)$.

The above Theorem 4.2 gives the boundary for the k for a possible extinction of E^k if

$$k_T > \frac{m}{b_0(e_y - hm)}. \tag{4.6}$$

This phenomenon significantly impacts the consumer population. When k exceeds the critical bifurcation value, the resource-only equilibrium E^k becomes the sole stable state, leading to consumer extinction. Additionally, condition (4.6) highlights that factors like the consumer's minimum attack rate (b_0), mortality rate (m), and conversion efficiency (e) are crucial for the persistence and survival of the consumer population.

5. Numerical results. In this section, we perform numerical simulations to corroborate the theoretical results and explore key dynamical features of system (2.3). Figures 6 and 7 present the sensitivity heat map (SHM) and parameter sensitivity analysis (PSA) for the resource (x) and consumer (y) populations with respect to various parameters. The SHM and PSA effectively assess model sensitivity, illustrating how perturbations in parameter space influence state variables. The SHM groups parameter sensitivities for each state variable, while the PSA quantifies the sensitivity of output state variables to individual parameters. These methods leverage the property that perturbations in high-dimensional parameter space often produce low-dimensional changes in output variables [14]. Figure 6 shows the SHM under stable and oscillatory coexistence conditions. Positive values indicate that the relative change in the parameter leads to a rise in population density, while negative values

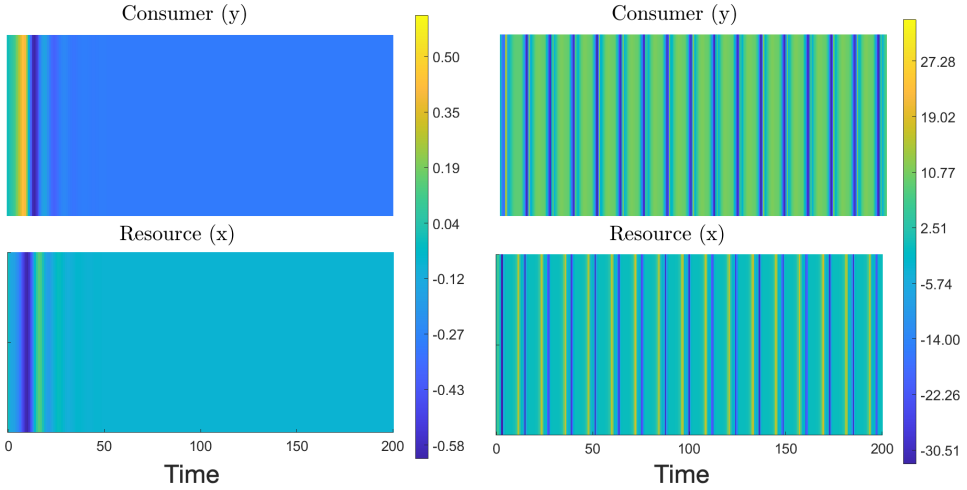

(a) (b)

FIG. 6. *SHM for the model* (2.3) (a) *under a stable coexistence condition and* (b) *under an oscillatory coexistence condition.*

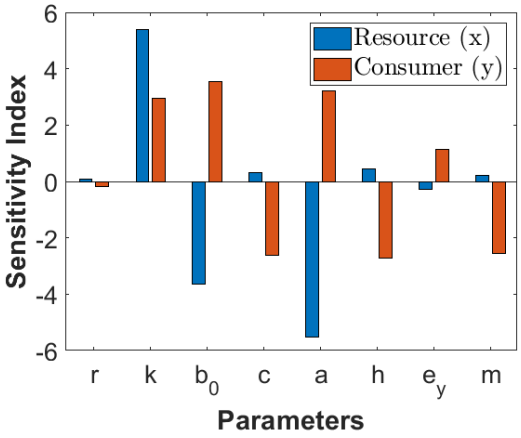

FIG. 7. *Local sensitivity analysis of model* (2.3).

suggest a decline. In the stable coexistence scenario (Figure 6(a)), parameter-induced density changes occur primarily during the initial transient phase, after which the system stabilizes and becomes less sensitive. In contrast, the oscillatory coexistence case (Figure 6(b)) shows periodic fluctuations in sensitivity, corresponding to the cyclical nature of the population dynamics. Overall, the consumer population demonstrates greater sensitivity to parameter changes than the resource population, indicating a stronger density response to perturbations. Figure 7 analyzes the sensitivity of output state variables to individual parameters, highlighting their influence on resource and consumer dynamics. The consumer population is particularly sensitive to the minimum attack rate (b_0), where small changes significantly affect its dynamics. The carrying capacity (k) and predation rate (a) positively influence the consumer population, with k also playing a key role in resource growth. Higher consumer mortality rates (m) negatively impact the consumer population size. This analysis identifies b_0, k, a, and m as critical drivers of system behavior and stability.

To investigate the effect of the consumer mortality rate (m), we vary the parameter m while keeping all other parameters fixed as in Table 1. For very low values of m, the system exhibits an interior positive equilibrium E^*, which corresponds to a stable limit cycle, and a boundary equilibrium E^k, which behaves as a saddle point (see Figure 8(a)). As the mortality rate m increases, the amplitude of the limit cycle declines, and at $m = 0.35$ (denoted as m_{Hopf}), the limit cycle disappears. At this point, the system transitions to a stable interior equilibrium E_1^*. To confirm the occurrence of a Hopf bifurcation at $m = m_{Hopf}$, we verify the condition: $(\frac{d\mathrm{Re}(\lambda)}{dm})_{m=m_{Hopf}} = -0.028$. This condition ensures that a limit cycle exists for $m < m_{Hopf}$. According to Theorem 4.1, the system undergoes a Hopf bifurcation at $m = m_{Hopf}$. The first Lyapunov coefficient is calculated as $l_1 = -0.39$, indicating that the Hopf bifurcation is supercritical and that the bifurcated limit cycle Γ_1 is stable. For $m > m_{Hopf}$, the system stabilizes at the interior equilibrium E^*. As m continues to increase, the system reaches a critical threshold $m_T = 0.45$, where a bistable behavior emerges between the equilibria E^* and E^k. At $m = m_{fold}$, the system undergoes a saddle-node bifurcation, leaving E^k as the only remaining equilibrium, which becomes globally stable. From an ecological perspective, at low mortality rates, the system supports coexistence, with resource and consumer populations exhibiting oscillations (limit cycles). As mortality

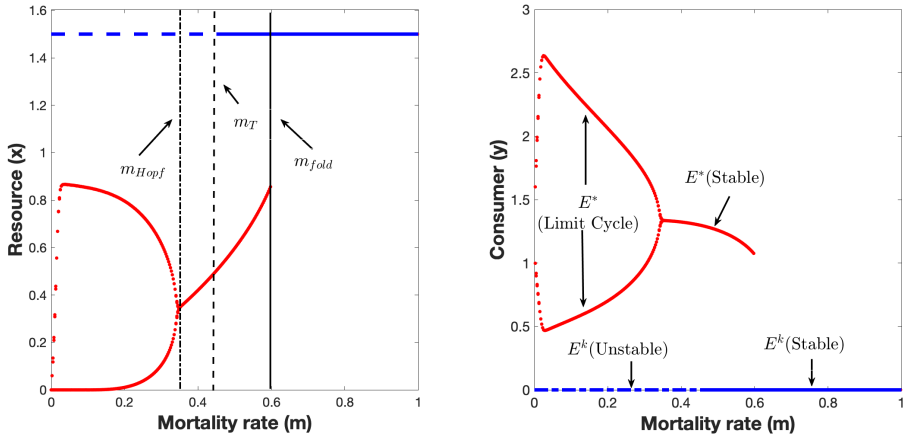

(a)

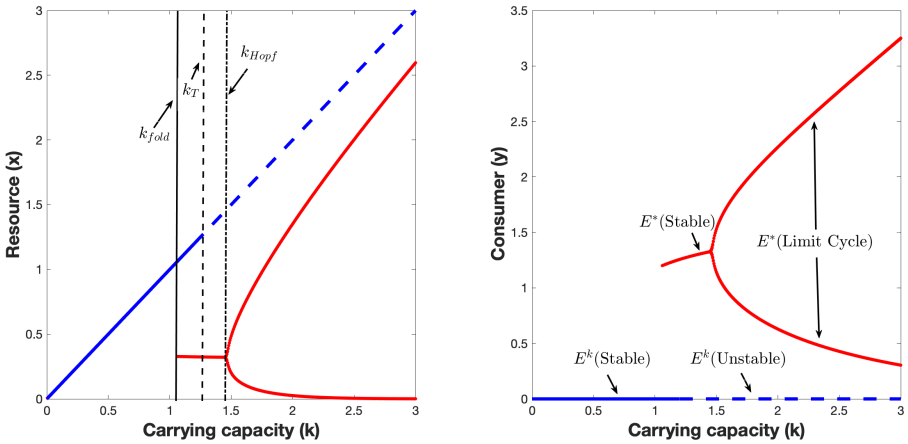

(b)

FIG. 8. *Bifurcation diagram of internal positive equilibrium* (E^*) *for the model* (2.3) *for* $b_0 = 0.5$*:* (a) *variation with mortality rate* (m)*;* (b) *variation with carrying capacity* (k)*. The corresponding equilibrium labels shown in the right panels also apply to the left panels.*

increases, the consumer population declines, and the system stabilizes at an interior equilibrium. Further increases in mortality lead to the extinction of the consumer population, leaving only a stable resource equilibrium.

To examine the effect of food supply through the carrying capacity (k) in our model, we fix $b_0 = 0.5$ and keep all other parameters the same as in Table 1. Figure 8(b) presents bifurcation diagrams for the consumer-resource system. For lower values of k, the system exhibits a boundary equilibrium point E^k, which is asymptotically stable, up to $k = 1.2$ (denoted as k_{fold}), where a fold bifurcation occurs. Beyond this point, both the boundary and interior equilibrium points coexist and remain stable until they collide. For $k > k_T$, the boundary equilibrium points disappear. At $k = 1.5$ (denoted as k_{Hopf}), the system undergoes a Hopf bifurcation, leading to

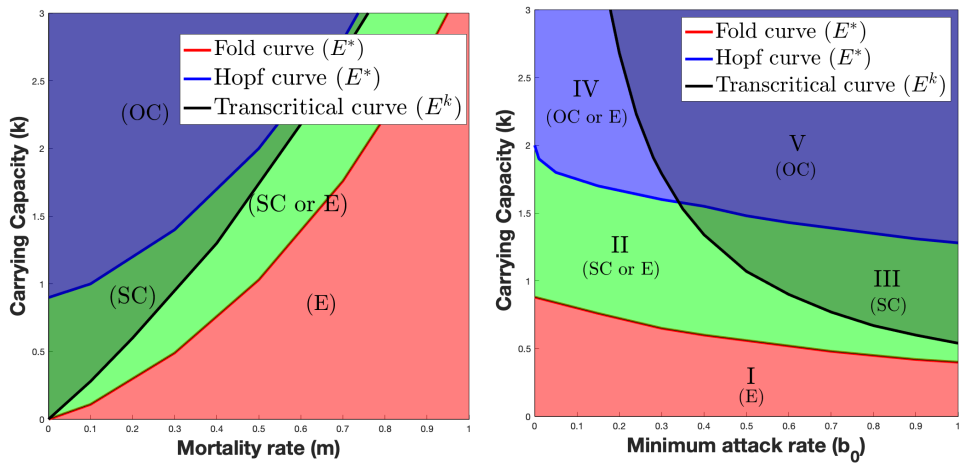

(a) (b)

FIG. 9. *Two-parameter bifurcation diagram of model* (2.3) *showing the effects of resource carrying capacity* (k) *with* (a) *consumer mortality rate* (m) *at* $b_0 = 0.5$, (b) *minimum attack rate* (b_0) *at* $m = 0.33$. *Regions are labeled as E: extinction, SC: stationary coexistence, and OC: oscillatory coexistence.*

the emergence of a stable limit cycle, and the interior equilibrium point E_1^* becomes unstable. The amplitude of the limit cycle grows as the carrying capacity increases.

To analyze the combined effects of mortality rate (m) and carrying capacity (k) in our model, we vary m and k while keeping all other parameters fixed as in Table 1. The resulting behavior of the system allows the mk-plane to be partitioned into distinct regions, separated by three bifurcation curves: the fold curve (red), the Hopf curve (blue), and the transcritical curve (black) (see Figure 9(a)). (Color images are available online.) In the top-left region labeled (OC), the system exhibits oscillatory coexistence, where stable limit cycles emerge around the interior equilibrium E^*, indicating periodic dynamics between the consumer and resource populations. The corresponding phase portrait for $m = 0.33, k = 2$ is shown in Figure 10(e). Moving downward and rightward, the (SC) region represents stable coexistence, where the system stabilizes at an interior equilibrium E^*. The phase portrait for $m = 0.33, k = 1.2$ is presented in Figure 10(c). The intermediate region labeled (SC or E) lies between the fold and transcritical curves and represents bistability, where both a stable interior equilibrium and a boundary equilibrium coexist. The corresponding phase portrait for $m = 0.33, k = 0.5$ is shown in Figure 10(b). In the bottom-right region labeled (E), higher mortality rates (m) and lower carrying capacities (k) cause the consumer population to collapse, leaving only the resource population at the boundary equilibrium E^k. The corresponding phase portrait for $m = 0.33, k = 0.2$ is presented in Figure 10(a). The Hopf curve marks the transition where oscillatory dynamics emerge via a Hopf bifurcation, while the fold curve denotes the point where equilibria collide and disappear. The transcritical curve signals the shift between boundary and interior equilibria. Overall, this analysis demonstrates that increasing food supply (through higher k) or reducing consumer mortality (m) can promote coexistence, while higher mortality and limited food supply drive the system toward extinction dynamics.

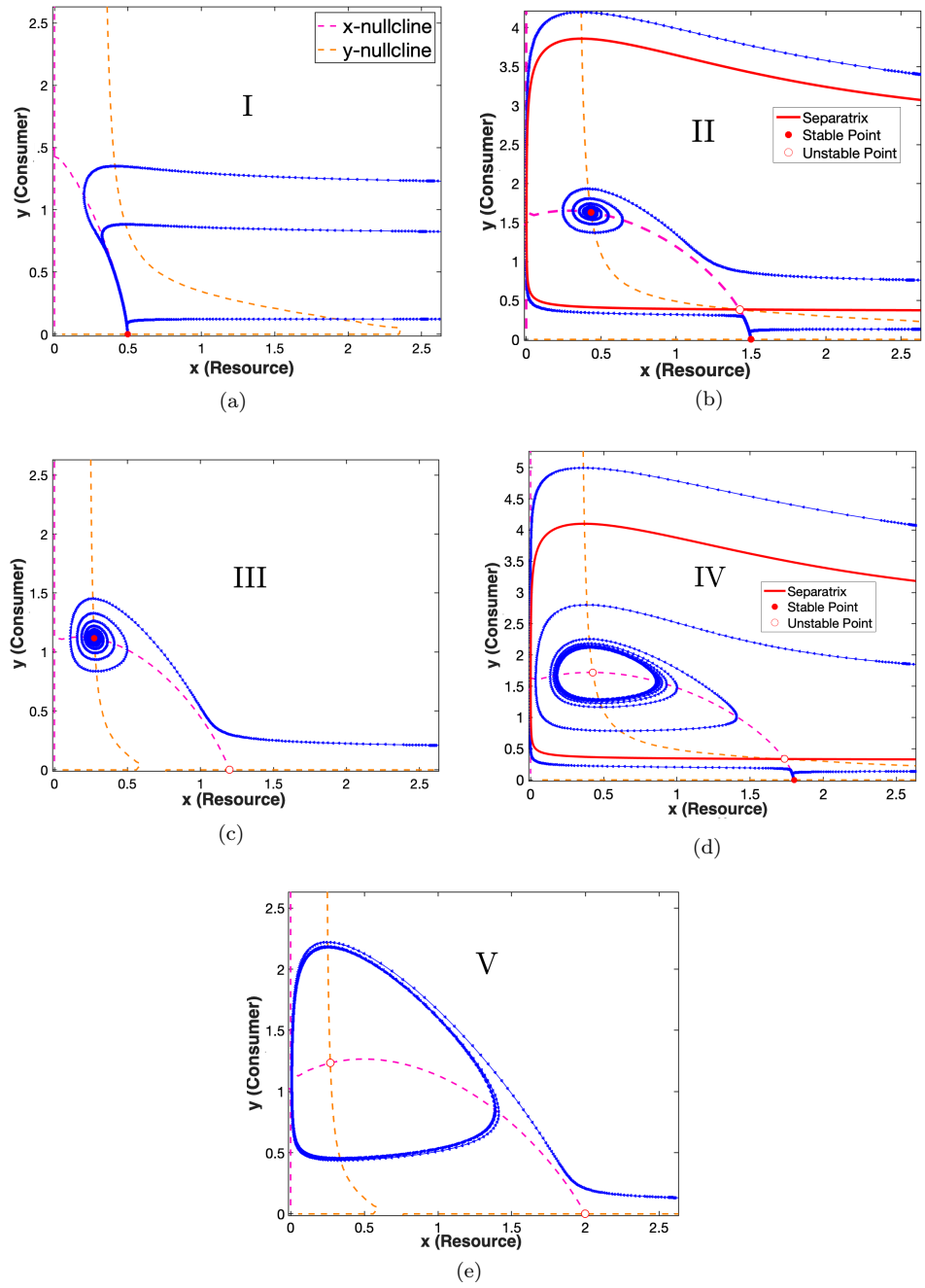

FIG. 10. *Phase portrait in each of the regions* $R_1 - R_5$ *shown in Figure* 9(b). *Parameters values are* (a) R_1*:* $b_0 = 0.2, k = 0.5$, (b) R_2*:* $b_0 = 0.1, k = 1.5$, (c) R_3*:* $b_0 = 0.8, k = 1.2$, (d) R_4*:* $b_0 = 0.1, k = 2.2$, (e) R_5*:* $b_0 = 0.5, k = 2$.

Figures 9(b) and 10 illustrate how the minimum attack rate b_0 and resource carrying capacity k shape the consumer-resource system dynamics. At low carrying capacity, regardless of the attack rate, the system undergoes population collapse

TABLE 2
Equilibrium dynamics across the regions shown in Figure 9(b).

Phase dynamics	E^k	E_1^*	E_2^*	**Remarks**
R_1 [Figure 10(a)]	Stable	-	-	E^k is asymptotically stable.
R_2 [Figure 10(b)]	Stable	Stable	Saddle	E^k and E_1^* are asymptotically stable.
R_3 [Figure 10(c)]	Saddle	Stable	-	E_1^* is asymptotically stable.
R_4 [Figure 10(d)]	Stable	Unstable	Saddle	E^k is asymptotically stable and there is a stable limit cycle around E_1^*.
R_5 [Figure 10(e)]	Saddle	Unstable	-	There is a stable limit cycle around E_1^*.

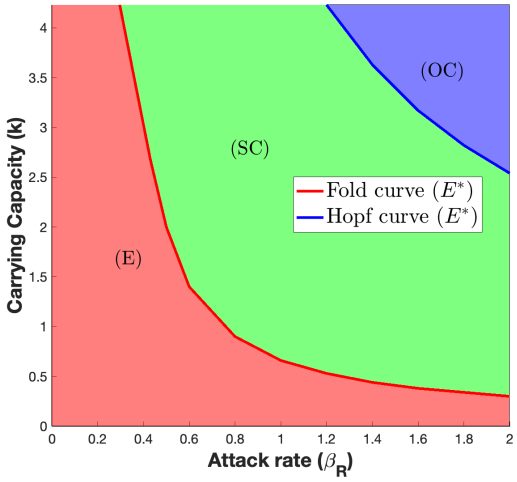

FIG. 11. *Two parameter bifurcation diagram of Rosenzweig–MacArthur model* (2.1) *for consumer carrying capacity* (k) *and attack rate* (β_R).

(Region I), where consumers fail to survive due to insufficient resources, leaving only the resource population [12]. At moderate values of k and attack rates, the system enters a bistable state (Region II), where the consumer population can coexist with the resource at an interior equilibrium or collapse to a boundary equilibrium, depending on initial conditions, where a minimum resource density is required to avoid extinction [11]. The resource density at the coexistence equilibrium increases with k, expanding the basin of attraction and promoting resource persistence. Crossing the transcritical bifurcation manifold (Region III) leads to stable coexistence, where resource growth and consumer consumption balance. At higher k and lower attack rates, oscillatory coexistence emerges (Regions IV and V). Here, the system exhibits periodic consumer-resource dynamics, where consumer populations rise with resource abundance and decline as resources deplete. The amplitude of these cycles increases with k, aligning with the paradox of enrichment. The fold, Hopf, and transcritical bifurcation curves mark critical thresholds between collapse, stable coexistence, and oscillations, providing insights into ecological balance and species persistence.

Table 2 summarizes the equilibria dynamics across regions R_1 to R_5, as illustrated in the bifurcation structure.

To compare the bifurcation structures of models (2.1) and (2.3), we present the bifurcation diagram of model (2.1) in Figure 11, illustrating how the resource

carrying capacity k and the attack rate parameter β_R affect the system dynamics. In the Rosenzweig–MacArthur model (2.1), the system exhibits three distinct regions: population collapse (E), stable coexistence (SC), and oscillatory coexistence (OC). At lower resource carrying capacities and higher attack rates, the system collapses to extinction (E), while higher carrying capacities allow stable coexistence or oscillations to emerge through a Hopf bifurcation. In contrast to model (2.3), which introduces more complexity with five regions (I, II, III, IV, and V), separated by fold, Hopf, and transcritical bifurcation curves. The additional dynamics include regions of bistability (II), where stable coexistence and population collapse coexist, and mixed oscillatory behavior (IV), where limit cycles or equilibrium points emerge depending on system parameters. The inclusion of a minimum attack rate b_0 further refines the behavior of the system, leading to richer dynamical results compared to the classical Rosenzweig–MacArthur model. Both models share similar fundamental behaviors (collapse, coexistence, and oscillations), while the new model captures additional ecological complexity, such as bistability and transitions influenced by both resource carrying capacity and attack rate parameters.

6. Discussion. The relationship between consumers and resources is a fundamental interaction that shapes ecosystems and influences population dynamics. Traditional mathematical approaches in behavioral and evolutionary ecology often focus on average behavior, neglecting individual differences and their functional significance in consumer-resource systems. Several studies have highlighted the impact of consumer behavior, particularly bold and shy strategies, on population dynamics [47, 15, 34]. Observations and empirical evidence across different trophic levels have provided valuable insights into behavioral interactions in real populations [26, 9, 21]. While empirical studies on animal behavior have garnered considerable attention, the role of behavioral variability in mathematical models remains underexplored. To address this gap, we propose a novel consumer-resource model (2.3) that incorporates consumer behavioral responses based on the ratio of resource and consumer densities. This model provides a framework for understanding how behavioral strategies influence population-level dynamics and resource consumption.

We examined the nonnegativity and boundedness of solutions for model (2.3), where the solutions are unique and remain nonnegative within the invariant set. Our analysis identified the conditions for different types of equilibria, showing that the resource-only equilibrium exists when the consumer's threshold consumption (C_0) is less than 1. Furthermore, we demonstrated that if the consumer's mortality rate exceeds the ratio of conversion efficiency to handling time, the interior equilibrium becomes stable, leading to the extinction of the consumer population regardless of its initial size. We derived conditions for the existence and nonexistence of positive steady states and observed that the system can exhibit either two positive equilibria or no positive equilibrium point.

In this study, we examined the core effects of boldness-mediated foraging behavior on consumer-resource dynamics, without introducing additional confounding factors. This simplification allowed us to focus on the behavioral feedback loop between food availability (modeled via the carrying capacity k) and consumer effort (influenced by the baseline boldness level b_0). Our analysis focuses on the coexistence equilibria and the bifurcations they undergo for specific parameter values, including fold, Hopf, and transcritical bifurcations. We derived the necessary and sufficient conditions for these bifurcations and provided formulae describing the bifurcation manifolds for a system with a general encounter rate function, which, to the best of our knowledge,

TABLE 3
Survival status of the consumer at different levels of food and aggressiveness.

Food supply→ Aggressiveness ↓	**Low**	**Moderate**	**High**
Low	Model (2.1): E Model (2.3): E	Model (2.1): E Model (2.3): E/SE	Model (2.1): E Model (2.3): E/OE
Moderate	Model (2.1): E Model (2.3): E	Model (2.1): E Model (2.3): E/SE	Model (2.1): SE Model (2.3): OE
High	Model (2.1): E Model (2.3): E	Model (2.1): SE Model (2.3): SE	Model (2.1): OE* Model (2.3): OE

E: extinction; SE: stable existence; OE: oscillatory existence.
* Needs more food supply.

has not been studied before. The bifurcation analysis reveals that consumer foraging aggressiveness is generally beneficial for the consumer population, which aligns with empirical studies. However, we found that when resource densities are low, increased foraging aggressiveness can lead to consumer extinction, with the critical resource density threshold determined by the fold bifurcation manifold (4.2). This finding aligns with previously published results [11], highlighting the risks of bold behavior under resource scarcity.

The inclusion of behavioral dynamics enhances the system described by model (2.3), producing richer and more complex dynamics compared to the Rosenzweig–MacArthur model (2.1). Table 3 highlights the differences between the two models in predicting consumer survival under varying food availability and aggressiveness. Biologically, at low food supply, both models predict consumer extinction due to insufficient resources. Under moderate food supply, model (2.1) still leads to extinction, while model (2.3) supports stable consumer survival or oscillatory dynamics at higher levels of aggressiveness, showcasing the role of behavioral variation. At high food supply, model (2.1) predicts oscillatory survival only when aggressiveness is high and requires additional food input for persistence. In contrast, model (2.3) consistently supports consumer survival through stable or oscillatory dynamics, even under varying levels of aggressiveness. These findings indicate that model (2.3) better incorporates the influence of behavioral traits, such as boldness and aggressiveness, along with resource availability on consumer persistence and population stability. Overall, under moderate food supply, a higher rate of consumer boldness emerges as the most advantageous and stable strategy for survival.

In this paper, we focused on a personality-driven consumer-resource model. However, consumer-resource interactions in natural communities are far more complex. For example, intraspecific competition among consumers is frequently observed [8], and intense competition can lead to the exclusion or extinction of weaker individuals or species. Additionally, studies have shown that consumer foraging behavior is strongly influenced by the presence of predation risk [45, 5]. Furthermore, consumer behavioral responses are also shaped by internal factors such as their fitness state, size, and age [43]. Incorporating these additional factors into future research could provide a more comprehensive and realistic understanding of consumer-resource dynamics and highlight the role of animal personality in shaping ecological communities.

Appendix A. Details of the data fitting. In the NLS approach, we assume that the x and y coordinates of the data are exact, but the corresponding functional response values may contain noise or distortions. The goal is to fit a solution curve

through the data such that the sum of the squares of the vertical distances between the observed data points and the curve is minimized. This distance is referred to as the least-squares error. Next, we illustrate how to use the NLS method to estimate unknown parameters.

Step 1. *Data collection.* In particular, suppose we are fitting the functional response $f(x, y)$ with the given data points

$$\{(x_1, y_1, \hat{f}_1), (x_2, y_2, \hat{f}_2), \ldots, (x_n, y_n, \hat{f}_n)\}.$$

Step 2. *NLS fitting.* The basic problem is to determine the set of parameters θ that minimizes the following sum-of-squares error (SSE):

$$\text{SSE}(\theta) = \min_{\theta} \sum_{i=1}^{n} \left\{ f(x_i, y_i, \theta) - \hat{f}(x_i, y_i) \right\}^2, \tag{A.1}$$

where $f(x_i, y_i, \theta)$ represents the functional response at (x_i, y_i) with parameter θ and $\hat{f}(x_i, y_i)$ represents the data of functional response at (x_i, y_i).

Step 3. *Solve the NLS problem numerically.* We use a MATLAB function `fminsearch` which takes the least-squares error function $\text{SSE}(\theta)$ and an initial guess of the parameter value θ_0 and uses a direct search routine to find a minimum value of least-squares error.

Step 4. *Compute confidence intervals.* We compute the approximate $100(1-\alpha)\%$ confidence intervals for each parameter given by

$$\theta \pm t_{\alpha/2,\, n-p} \cdot \sqrt{\frac{\text{SSE}(\hat{\theta})}{n-p} \cdot [(J^\top J)^{-1}]}, \tag{A.2}$$

where $t_{\alpha/2,\, n-p}$ is the critical value from the student's t-distribution with $n-p$ degrees of freedom, p is the number of parameters, and n is the number of data points. J is the Jacobian matrix evaluated at θ.

The parameters $\theta = (b_0, a, c, h)$ are estimated using field experiment data involving herbivorous fish and their resource, algae, collected from a near-pristine reef ecosystem [16]. Most of the initial parameter values are derived from existing literature [32, 6], except for those related to (2.4). The estimated parameters for model (2.3) are summarized in Table 1.

Appendix B. Details of the fold bifurcation. Here, we demonstrate that if a coexistence equilibrium of model (2.3) exists, then the condition (4.1) is equivalent to the Jacobian of the model having one zero eigenvalue when evaluated at this equilibrium. To proceed, we define a function $\mathcal{G}(x, y)$ such that $f(x, y) = x\mathcal{G}(x, y)$, where $f(x, y)$ represents the consumer functional response given in (2.5). Additionally, let $\mathcal{A}$ denote the Jacobian of model (2.3) and $[x^*, y^*]$ represent any coexistence equilibrium of this system. By direct computation, we obtain

$$\mathcal{A} = \begin{pmatrix} r - r\dfrac{2x^*}{k} - y^*\mathcal{G} - y^*x^*\mathcal{G}_x & -x^*\mathcal{G} - y^*x^*\mathcal{G}_y \\ e_y y^*\mathcal{G} + e_y y^* x^* \mathcal{G}_x & e_y x^*\mathcal{G} + e_y y^* x^* \mathcal{G}_y - m \end{pmatrix}, \tag{B.1}$$

where $\mathcal{G} = \mathcal{G}(x^*, y^*)$, $\mathcal{G}_x = \partial\mathcal{G}(x^*, y^*)/\partial x$, and $\mathcal{G}_y = \partial\mathcal{G}(x^*, y^*)/\partial y$. Since for the coexistence equilibrium $e_y x^* \mathcal{G} = m$, we get

$$\text{Tr } \mathcal{A} = r - r\frac{2x^*}{k} - y^*\mathcal{G} - y^*x^*\mathcal{G}_x + e_y y^* x^* \mathcal{G}_y, \tag{B.2}$$

$$\text{Det}\mathcal{A} = r\left(1 - \frac{2x^*}{k}\right) e_y y^* x^* \mathcal{G}_y + m y^* \mathcal{G} + \frac{m^2}{e_y} y^* \mathcal{G}_x. \tag{B.3}$$

Since the functional response implies $\mathcal{G}(x,y) = \frac{\beta(x,y)}{1+h\beta(x,y)x}$, we have

$$\mathcal{G}_x = -\mathcal{G}^2 h \quad \text{and} \quad \mathcal{G}_y = \frac{\Lambda \mathcal{G}^2}{\Lambda^2},$$

where $\Lambda(y^*) := \beta(x^* \in (0,k), y^*)$ with $x^* \in (0,k)$ with $k > 0$. Substituting $\mathcal{G}_x$, $\mathcal{G}_x$, and (3.3) into (B.3), we get

$$\text{Det}\mathcal{A} = y^* \mathcal{G} m \left(r\left(1 - \frac{2L_2}{\Lambda}\right)\frac{\Lambda}{\Lambda^2} + \frac{e_y - hm}{e_y} \right). \tag{B.4}$$

As a result, condition (4.1) is equivalent to the condition $\det \mathcal{A} = 0$ at a coexistence equilibrium $[x^*, y^*]$, which serves as a necessary condition for this equilibrium to be a limit point.

Appendix C. Details of Hopf bifurcation. For a Hopf bifurcation to occur at a parameter value in a two-dimensional system, real parts of the complex eigenvalues of the Jacobian evaluated at the respective system equilibrium have to transversally cross zero (i.e., change sign) when the parameter crosses that value. Denoting by a the bifurcation parameter and by $\lambda_r(a) \pm i\lambda_i(a)$ the respective pair of complex eigenvalues, we require $\lambda_r(a_c) = 0$, $\lambda_i(a_c) > 0$, and $\lambda_r'(a_c) \neq 0$ at a bifurcation point $a = a_c$ as necessary conditions for a Hopf bifurcation to occur. We note that

$$\lambda_r(a) = \frac{\text{Tr } \mathcal{A}(a)}{2} \quad \text{and} \quad \lambda_i(a) = \text{Det } \mathcal{A}(a),$$

where $\mathcal{A}(a)$ denotes the Jacobian evaluated at the system equilibrium corresponding to the parameter a.

Now we will prove that if a coexistence equilibrium of the model (2.3) exists, then condition (4.3) is necessary and sufficient for vanishing of the trace of the Jacobian of the model (2.3) at that equilibrium. Denoting $\mathcal{G}(x,y) = f(x,y)/x$, then at the coexistence equilibrium, we have

$$y^*\mathcal{G} = r\left(1 - \frac{x^*}{k}\right).$$

Consequently, at this equilibrium, the trace (B.2) of the Jacobian of the model (2.3) simplifies to

$$\text{tr } \mathcal{A} = -r\frac{x^*}{k} + r\left(1 - \frac{x^*}{k}\right) x^* \mathcal{G}\left(h + e_y \frac{\Lambda'}{\Lambda^2}\right).$$

Since $r > 0$ and according to (3.3) $\frac{x^*}{k} = \frac{L_2}{\Lambda} > 0$ at the coexistence equilibrium, we have

$$\text{tr } \mathcal{A} = -r\frac{x^*}{k}\left(1 + k\left(\frac{L_2}{\Lambda} - 1\right) g\left(h + e_y \frac{\Lambda'}{\Lambda^2}\right)\right),$$

where $L_2 = \frac{m}{k(e_y - hm)}$. Since the model (2.3) implies $\mathcal{G} = \frac{r\Lambda}{L_1}$, a necessary and sufficient condition for vanishing of the trace of the Jacobian of the model (2.3) at the coexistence equilibrium is

$$e\Lambda^2 = (k(e_y - hm)\Lambda - m)(h\Lambda^2 + e_y\Lambda'),$$

which is equivalent to the condition (4.3). Similar manipulation with the expression (B.4) and replacement of Λ' gives the second necessary condition (4.4).

The sign of the first Lyapunov coefficient determines the direction of the Hopf bifurcation, which is given by

$$\begin{aligned} l_1 = \frac{1}{16}\left[\frac{\partial^3 H_1}{\partial z_1^3} + \frac{\partial^3 H_1}{\partial z_1 \partial z_2^2} + \frac{\partial^3 H_2}{\partial z_1^2 \partial z_2} + \frac{\partial^3 H_2}{\partial z_2^3}\right] \\ + \frac{1}{16\omega}\left[\frac{\partial^2 H_1}{\partial z_1 \partial z_2}\left(\frac{\partial^2 H_1}{\partial z_1^2} + \frac{\partial^2 H_1}{\partial z_2^2}\right) - \frac{\partial^2 H_2}{\partial z_1 \partial z_2}\left(\frac{\partial^2 H_2}{\partial z_1^2} + \frac{\partial^2 H_2}{\partial z_2^2}\right)\right. \\ \left. - \frac{\partial^2 H_1}{\partial z_1 \partial z_2}\frac{\partial^2 H_2}{\partial z_1^2} + \frac{\partial^2 H_1}{\partial z_2^2}\frac{\partial^2 H_2}{\partial z_2^2}\right]. \end{aligned}$$

The higher-order terms $H_1(z_1, z_2)$ and $H_2(z_1, z_2)$ are given by

$$\begin{aligned} H_1(z_1, z_2) &= \frac{1}{a_{01}}\left[a_{20}a_{01}z_1^2 - a_{11}a_{01}z_1z_2 + a_{02}(a_{10}z_1 + \omega z_2)^2 + a_{03}(a_{10}z_1 + \omega z_2)^3\right], \\ H_2(z_1, z_2) &= -\frac{1}{a_{01}\omega}(a_{10}(a_{20}a_{01}z_1^2 - a_{11}a_{01}z_1z_2 + a_{02}(a_{10}z_1 + \omega z_2)^2 + a_{03}(a_{10}z_1 + \omega z_2)^3) \\ &\quad + b_{20}a_{01}z_1^2 - b_{11}a_{01}z_1z_2 + b_{02}(a_{10}z_1 + \omega z_2)^2 + b_{03}(a_{10}z_1 + \omega z_2)^3). \end{aligned}$$

Remark C.1. A similar analysis of Hopf bifurcation can be done for the other parameters.

REFERENCES

[1] K. A. Adeli, S. J. Woods, S. J. Cooke, and C. K. Elvidge, *Boldness and exploratory behaviors differ between sunfish (Lepomis spp.) congeners in a standardized assay*, Behav. Ecol. Sociobiol., 78 (2024), 46, https://doi.org/10.1007/s00265-024-03464-5.

[2] B. Adriaenssens and J. I. Johnsson, *Natural selection, plasticity and the emergence of a behavioural syndrome in the wild*, Ecol. Lett., 16 (2013), pp. 47–55, https://doi.org/10.1111/ele.12011.

[3] P. A. Biro and J. A. Stamps, *Are animal personality traits linked to life-history productivity?*, Trends Ecol. Evol., 23 (2008), pp. 361–368, https://doi.org/10.1016/j.tree.2008.04.003.

[4] M. Briffa and A. Weiss, *Animal personality*, Curr. Biol., 20 (2010), pp. R912–R914, https://doi.org/10.1016/j.cub.2010.09.019.

[5] D. A. Burkholder, M. R. Heithaus, and J. W. Fourqurean, *Patterns of top-down control in a seagrass ecosystem: Could a roving apex predator induce a behavior-mediated trophic cascade?*, J. Anim. Ecol., 82 (2013), pp. 1192–1202, https://doi.org/10.1111/1365-2656.12097.

[6] L. Capitani, N. Roos, G. O. Longo, R. Angelini, and L. Schenone, *Resource-to-consumer ratio determines the functional response of an herbivorous fish in a field experiment*, Oikos, 130 (2021), pp. 2100–2110, https://doi.org/10.1111/oik.08784.

[7] P. Chesson, *Mechanisms of maintenance of species diversity*, Annu. Rev. Ecol. Syst., 31 (2000), pp. 343–366, https://doi.org/10.1146/annurev.ecolsys.31.1.343.

[8] M. E. Clark, T. G. Wolcott, D. L. Wolcott, and A. H. Hines, *Intraspecific interference among foraging blue crabs Callinectes sapidus: Interactive effects of predator density and prey patch distribution*, Mar. Ecol. Prog. Ser., 178 (1999), pp. 69–78, https://doi.org/10.3354/meps178069.

[9] E. F. Cole and J. L. Quinn, *Shy birds play it safe: Personality in captivity predicts risk responsiveness during reproduction in the wild*, Biol. Lett., 10 (2014), 20140178, https://doi.org/10.1098/rsbl.2014.0178.
[10] J. L. Conrad, K. L. Weinersmith, T. Brodin, J. B. Saltz, and A. Sih, *Behavioural syndromes in fishes: A review with implications for ecology and fisheries management*, J. Fish Biol., 78 (2011), pp. 395–435, https://doi.org/10.1111/j.1095-8649.2010.02874.x.
[11] F. Courchamp, L. Berec, and J. Gascoigne, *Allee Effects in Ecology and Conservation*, Oxford University Press, Oxford, 2008.
[12] S. Creel and N. M. Creel, *Communal hunting and pack size in African wild dogs, Lycaon pictus*, Anim. Behav., 50 (1995), pp. 1325–1339, https://doi.org/10.1016/0003-3472(95)80048-4.
[13] S. R. X. Dall, A. I. Houston, and J. M. McNamara, *The behavioural ecology of personality: Consistent individual differences from an adaptive perspective*, Ecol. Lett., 7 (2004), pp. 734–739, https://doi.org/10.1111/j.1461-0248.2004.00618.x.
[14] M. Domijan, P. E. Brown, B. V. Shulgin, and D. A. Rand, *PeTTSy: A computational tool for perturbation analysis of complex systems biology models*, BMC Bioinform., 17 (2016), 124, https://doi.org/10.1186/s12859-016-0972-2.
[15] C. P. dos Santos, M. N. de Oliveira, P. F. Silva, and A. C. Luchiari, *Relationship between boldness and exploratory behavior in adult zebrafish*, Behav. Process., 209 (2023), 104885, https://doi.org/10.1016/j.beproc.2023.104885.
[16] M. A. Gil, M. L. Baskett, S. B. Munch, and A. M. Hein, *Fast behavioral feedbacks make ecosystems sensitive to pace and not just magnitude of anthropogenic environmental change*, Proc. Natl. Acad. Sci. USA, 117 (2020), pp. 25580–25589, https://doi.org/10.1073/pnas.2003301117.
[17] S. D. Gosling, *From mice to men: What can we learn about personality from animal research?*, Psychol. Bull., 127 (2001), pp. 45–86, https://doi.org/10.1037/0033-2909.127.1.45.
[18] A. Hastings, *Population Biology: Concepts and Models*, Springer, New York, 1997.
[19] K. Hulthén, B. B. Chapman, P. A. Nilsson, J. Hollander, C. Brönmark, C. Skov, L.-A. Hansson, and J. Brodersen, *A predation cost to bold fish in the wild*, Sci. Rep., 7 (2017), 1239, https://doi.org/10.1038/s41598-017-01270-w.
[20] R. Kortet, A. V. Hedrick, and A. Vainikka, *Parasitism, predation and the evolution of animal personalities*, Ecol. Lett., 13 (2010), pp. 1449–1458, https://doi.org/10.1111/j.1461-0248.2010.01536.x.
[21] R. H. J. M. Kurvers, V. M. A. P. Adamczyk, S. E. van Wieren, and H. H. T. Prins, *The effect of boldness on decision-making in barnacle geese is group-size-dependent*, Proc. Roy. Soc. B Biol. Sci., 278 (2011), pp. 2018–2024, https://doi.org/10.1098/rspb.2010.2266.
[22] S. L. Lima and L. M. Dill, *Behavioral decisions made under the risk of predation: A review and prospectus*, Can. J. Zool., 68 (1990), pp. 619–640, https://doi.org/10.1139/z90-092.
[23] A. J. Lotka, *Elements of Physical Biology*, Williams and Wilkins, Baltimore, MD, 1925.
[24] B. Luttbeg and A. Sih, *Risk, resources, and state-dependent adaptive behavioural syndromes*, Philos. Trans. B, 365 (2010), pp. 3977–3990, https://doi.org/10.1098/rstb.2010.0207.
[25] J. Malard, J. Adamowski, J. B. Nassar, N. Anandaraja, H. Tuy, and H. Melgar-Quiñonez, *Modelling predation: Theoretical criteria and empirical evaluation of functional form equations for predator-prey systems*, Ecol. Model., 437 (2020), 109264, https://doi.org/10.1016/j.ecolmodel.2020.109264.
[26] G. G. Mittelbach, N. G. Ballew, and M. K. Kjelvik, *Fish behavioral types and their ecological consequences*, Can. J. Fish. Aquat. Sci., 71 (2014), pp. 927–944, https://doi.org/10.1139/cjfas-2013-0558.
[27] W. W. Murdoch, C. J. Briggs, and R. M. Nisbet, *Consumer-Resource Dynamics*, Princeton University Press, Princeton, NJ, 2003.
[28] R. T. Paine, *Food web complexity and species diversity*, Amer. Natural., 100 (1966), pp. 65–75, https://doi.org/10.1086/282400.
[29] L. Perko, *Differential Equations and Dynamical Systems*, Springer, New York, 2013.
[30] J. N. Pruitt and A. P. Modlmeier, *Animal personality in a foundation species drives community divergence and collapse in the wild*, J. Anim. Ecol., 84 (2015), pp. 1461–1468, https://doi.org/10.1111/1365-2656.12406.
[31] D. Réale, S. M. Reader, D. Sol, P. T. McDougall, and N. J. Dingemanse, *Integrating animal temperament within ecology and evolution*, Biol. Rev., 82 (2007), pp. 291–318, https://doi.org/10.1111/j.1469-185X.2007.00010.x.
[32] M. L. Rosenzweig and R. H. MacArthur, *Graphical representation and stability conditions of predator-prey interactions*, Amer. Natural., 97 (1963), pp. 209–223, https://doi.org/10.1086/282272.

[33] P. C. de Ruiter, V. Wolters, J. C. Moore, and K. O. Winemiller, *Food web ecology: Playing Jenga and beyond*, Science, 309 (2005), pp. 68–71, https://doi.org/10.1126/science.1096112.

[34] E. Sales, L. Rogers, R. Freire, O. Luiz, and R. K. Kopf, *Bold-shy personality traits of globally invasive, native and hatchery-reared fish*, Roy. Soc. Open Sci., 10 (2023), 231035, https://doi.org/10.1098/rsos.231035.

[35] S. Shiratsuru, Y. N. Majchrzak, M. J. L. Peers, E. K. Studd, A. K. Menzies, R. Derbyshire, M. M. Humphries, C. J. Krebs, D. L. Murray, and S. Boutin, *Food availability and long-term predation risk interactively affect antipredator response*, Ecology, 102 (2021), e03456, https://doi.org/10.1002/ecy.3456.

[36] A. Sih, A. M. Bell, and J. C. Johnson, *Behavioral syndromes: An ecological and evolutionary overview*, Trends Ecol. Evol., 19 (2004), pp. 372–378, https://doi.org/10.1016/j.tree.2004.04.009.

[37] A. Sih, J. Cote, M. Evans, S. Fogarty, and J. Pruitt, *Ecological implications of behavioural syndromes*, Ecol. Lett., 15 (2012), pp. 278–289, https://doi.org/10.1111/j.1461-0248.2011.01731.x.

[38] G. T. Skalski and J. F. Gilliam, *Functional responses with predator interference: Viable alternatives to the holling type* II *model*, Ecology, 82 (2001), pp. 3083–3092, https://doi.org/10.1890/0012-9658(2001)082[3083:FRWPIV]2.0.CO;2.

[39] J. A. Stamps, *Growth-mortality tradeoffs and personality traits in animals*, Ecol. Lett., 10 (2007), pp. 355–363, https://doi.org/10.1111/j.1461-0248.2007.01034.x.

[40] D. B. Stouffer and M. Novak, *Hidden layers of density dependence in consumer feeding rates*, Ecol. Lett., 24 (2021), pp. 520–532, https://doi.org/10.1111/ele.13670.

[41] W. J. Sutherland, L. V. Dicks, N. Ockendon, and R. K. Smith, eds., *What Works in Conservation?*, Open Book Publishers, Cambridge, UK, 2013.

[42] D. Tilman, *Resource Competition and Community Structure*, Princeton University Press, Princeton, NJ, 1982.

[43] C. N. Toms, D. J. Echevarria, and D. J. Jouandot, *A methodological review of personality-related studies in fish: Focus on the shy-bold axis of behavior*, Int. J. Comparative Psychol., 23 (2010), pp. 1–25, https://doi.org/10.46867/IJCP.2010.23.01.08.

[44] B. J. Toscano and B. D. Griffen, *Trait-mediated functional responses: Predator behavioural type mediates prey consumption*, J. Anim. Ecol., 83 (2014), pp. 1469–1477, https://doi.org/10.1111/1365-2656.12236.

[45] G. C. Trussell, P. J. Ewanchuk, and M. D. Bertness, *Trophic cascades in rocky shore pools: Distinguishing lethal and non-lethal effects*, Oecologia, 139 (2004), pp. 427–432, https://doi.org/10.1007/s00442-004-1512-8.

[46] T. M. Vignaud, C. G. Meyer, C. Séguigne, J. Bierwirth, and E. E. Clua, *Examining individual behavioural variation in wild adult bull sharks (Carcharhinus leucas) suggests divergent personalities*, Behaviour, 160 (2023), pp. 1283–1301, https://doi.org/10.1163/1568539X-bja10244.

[47] A. D. M. Wilson and E. D. Stevens, *Consistency in context-specific measures of shyness and boldness in rainbow trout, oncorhynchus mykiss*, Ethology, 111 (2005), pp. 849–862, https://doi.org/10.1111/j.1439-0310.2005.01110.x.

[48] M. Wolf and F. J. Weissing, *Animal personalities: Consequences for ecology and evolution*, Trends Ecol. Evol., 27 (2012), pp. 452–461, https://doi.org/10.1016/j.tree.2012.05.001.